5. Steinmetz, T., Wilken, T., Araujo-Hauck, C., Holzwarth, R., Hänsch, T. W., Pasquini, L., Manescau, A., D'Odorico, S., Murphy, M. T., Kentischer, T., Schmidt, W., Udem, Th. (2008). Laser frequency combs for astronomical observations. Science, 321 (5894), 1335–1337. doi: 10.1126/science.1161030

6. Li, C.-H., Benedick, A. J., Fendel, P., Glenday, A. G., Kärtner, F. X., Phillips, D. F., Sasselov, D., Szentgyorgyi, A., Walsworth, R. L. (2008). A laser frequency comb that enables radial velocity measurements with a precision of 1 cm s(-1). Nature, 452 (7187), 610–612. doi: 10.1038/nature06854

7. Li, H. (2007). Near-infrared diode laser absorption spectroscopy with applications to reactive system and combustion control. Submitted to the department of mechanical engineering and the committee on graduate studies of Stanford university, 166.

8. Li, S., Koscica, T., Zhang, Y., Li, D., Cui, H.-L. (2008). Optical fiber remote sensing system of methane at 1645nm using wavelength-modulation technique. Department of Physics and Engineering Physics , Stevens Institute of Technology.

9. Shimose, Y., Okamoto, T., Maruyama, A., Aizawa, M., Nagai, H. (1991). Remote sensing of methane gas by differential absorption measurement using a wavelength tunable DFB LD. IEEE Photonics Technology Letters, 3 (1), 86–87. doi: 10.1109/68.68057

10. Gamache, R. R., Kennedy, S., Hawkins, R., Rothman, L. S. (2000). Total internal partition sums for molecules in the terrestrial atmosphere. Journal of Molecular Structure, 517-518, 407–425. doi: 10.1016/s0022-2860(99)00266-5

11. Nagali, V., Hanson, R. K. (1997). Design of a diode-laser sensor to monitor water vapour in high-pressure combustion gases. Applied Optics, 36 (36), 9518–9527. doi: 10.1364/ao.36.009518

12. Chan, K., Ito, H., Inaba, H. (1984). An Optical-Fiber-Based Gas Sensor for Remote Absorption Measurement of Low-Level CH4 Gas in the Near-Infrared Region. Journal of Lightwave Technology, 2 (3), 234–237. doi: 10.1109/jlt.1984.1073609

**Haider Ali Muse**, Faculty of electronic engineering, Department of Physical Foundations of Electronic Engineering, Kharkiv national university of radio electronics, st. Lenina 14, Kharkov, 61000
Hadr_2005@yahoo.com

## AERODYNAMIC STATE DIAGNOSING METHOD OF AIRCRAFT WITH THERMAL FIELD USAGE

© V. Kazak, D. Shevchuk, A. Babenko, M. Levchenko

*The method of aerodynamic condition of the aircraft on the thermal fields was developed as a research result. Based on the mathematical and natural experiments, there are identified the regularities of formation of temperature gradients in the boundary layer of air that occurs after damage of external contours; there are detected parameters that affect the behavior of the temperature gradient arising from damage.*
*Keywords: external contour, damage, plane, aircraft, temperature gradient, thermal method, boundary layer, diagnostics.*

*В результаті проведених досліджень було розроблено метод аеродинамічного стану літака по теплових полях. На основі математичного та натурного експериментів, встановлено: закономірності формування температурного градієнту у прикордонному шарі повітря, що виникає за пошкодженням зовнішніх обводів; виявлено параметри, які впливають на поведінку температурного градієнту, що виникає за пошкодженням.*
*Ключові слова: зовнішні обводи, пошкодження, повітряний корабель, температурний градієнт, тепловий метод, прикордонний шар, діагностування.*

### 1. Introduction

The issue of safety, including reducing the number of aviation accidents with fatalities worldwide, regardless of the amount of air transportation is a primary objective of the international Civil Aviation Organization (ICAO: Global Aviation Safety Plan, 2011, Montreal, Canada). According to the Federal Aviation Administration USA (FAA) annually in civil aviation there are about five huge aircraft accidents in which an important role is played by the collision of aircraft with biological, mechanical or electrical forces. At the same time every year a growing number of aircraft collisions with external forces, due to several factors, namely the increasing intensity of operations and the increase in bird populations. In particular, the number of aircraft collisions with birds in flight over the period 2005–2013 biennium. Has almost doubled – from 36,000 to 70,000 cases of collision per year for all types of civil aviation [1–3].

Thus the danger of accidental injuries in the collision of aircraft with the above units is that the appearance of lesions can not be predicted or detected in a timely flight. Analysis of Accident Investigation showed that the highest probability of collision with mechanical, electrical and biological formations appears

on take-off and landing stage. In this regard, the recent research interest rise to developers for diagnostics of the outer contour of the aircraft in flight. Availability of timely, complete and accurate information about the time, place and degree of damage will objectively assess the nature of aviation accident and in accordance with this take the necessary steps to prevent its development through reorganization or change of flight mode control actions.

**2. Analysis of published data and the formulation of the problem**

Experts estimate that at the time of the collision impact force is proportional to the square of the speed of birds flying aircraft. Thus, a bird weighing less than 2 kg strikes the external contour of an airplane flying at a speed of 700 km/h, three times stronger than the bomb 50-millimeter cannon, and the force of impact of sea gulls at the speed of the airplane 900 km / h is about 270,000 N (27 tons). The bird can easily pierce fuselage skin and wings, thereby worsening the aerodynamics of aircraft, engine and get to deform or tear the rotor blade damage the glass cockpit. When hitting birds near the rivet joint plating last often collapses, and under the action of the velocity head damaged seam opens, causing further destruction of the power set [3].



Fig. 1. Cases of civilian aircraft collision with birds: *a, b* – the landing phase of flight; *c, d* – the stage of flight take off

**3. The purpose and objectives of the research**

Analysis of the factors causing damage to the external contour of the aircraft, as well as an analysis of accidents allows to distinguish three main groups of damages by reason of occurrence:

– collision with mechanical (radiosondes, balloons, transzondy and other means necessary to control the meteorological state of the atmosphere) or biological objects;

– electrostatic discharges and lightning;

– chemical processes occurring in the metal construction of aircraft as in contact with the surface of reactive substances and longer connected to the operating conditions of the aircraft (corrosion, aging and degradation of the metal, etc.).

By the time damage can be distinguished as a gradual or sudden. Gradual damage characterized by the presence of trends or patterns of change given the aerodynamic characteristics of the external contour of the aircraft at the time preceding the time of the fault. The cause of such damage is the effect of physical and chemical processes. Studying the laws of their development by means of predictive methods of diagnosis, we can predict their occurrence in the process of preparing the aircraft for operation, as well as for the technical inspection of the aircraft ground services at the airport or repair airlines.

Sudden damage characterized by an abrupt change in the value of one or more specified parameters. The change is caused by the action of physical or mechanical processes, the course of which is not controlled, to provide the appearance of such lesions is not possible. As the analysis of publications [4, 5], a significant number of accidents was caused precisely by sudden structural damage to the aircraft. Therefore there is a need to develop methods of diagnosing the external contour of the aircraft in order to identify the date, place and degree

of damage, as well as methods of preserving stability and control to prevent the development of an emergency in flight.

### 4. Materials and methods

During the movement of the aircraft along its surface boundary layer is formed – that is, isolated thin layer of air in which the speed is changed from 0 at the surface of the external contour to its full speed of the total flow [6, 7]. Thus there is an air particles sticking to the surface of the external contour in the direction of the incoming flow. This phenomenon is accompanied by heating the surface of the aircraft induced inhibition of the external contour of the air layer. Heating occurs due to friction and due to the adiabatic compression of air. Between the surface and the outer contours of the boundary layer occurs forced convective heat transfer, which is accompanied by the thermal conductivity.

When the two-dimensional flow around a system of equations of continuity and motion for the boundary layer of air flow, taking into account the compression and unsteadiness, has the form [8]:

$$\frac{\partial \rho}{\partial t} + \frac{\partial(\rho u)}{\partial x} + \frac{\partial(\rho \upsilon)}{\partial y} + \frac{\partial(\rho \omega)}{\partial z} = 0 , \quad (1)$$

$$\rho\left(\frac{\partial u}{\partial t} + \frac{\partial u}{\partial x} + \frac{\partial u}{\partial y}\right) = -\frac{\partial p}{\partial x} + \frac{\partial}{\partial y}\left(\mu \frac{\partial u}{\partial y}\right) \quad (2)$$

where x, y – the axis of a Cartesian coordinate system; $u, \upsilon$ – the projection of the vector flow velocity v along the axis; t – time; - Specific heat of air; $\rho$ – density of air; p – the pressure; T – temperature; $\mu$ – dynamic viscosity.

The energy conservation law for the two-dimensional air flow can be written as [8]:

$$\rho c_p\left(\frac{\partial T}{\partial t} + u\frac{\partial T}{\partial x} + \upsilon\frac{\partial T}{\partial y}\right) = \lambda\frac{\partial^2 T}{\partial y^2} + \mu\left(\frac{\partial u}{\partial y}\right)^2 + \frac{\partial p}{\partial t} + u\frac{dp}{dx}, (3)$$

where $\lambda$ – the thermal conductivity of air.

In the study of airflow damaged external contour must consider the three-dimensional case of flow. The law of conservation of energy in this case can be written as follows [8]:

$$\rho c_p \frac{DT}{Dt} = \frac{\partial}{\partial x}\left(\lambda\frac{\partial T}{\partial x}\right) + \frac{\partial}{\partial y}\left(\lambda\frac{\partial T}{\partial y}\right) + \frac{\partial}{\partial z}\left(\lambda\frac{\partial T}{\partial z}\right) - p(\nabla \cdot v) + \mu \Phi, (4)$$

where $\frac{DT}{Dt}$ – substantial derivative, $\Phi$ – dissipation function.

It is necessary to take into account the dependence of the physical properties of air parameters of thermodynamic parameters:

$$c_p = c_p(p, T) ; \lambda = \lambda(p, T) ;$$
$$\mu = \mu(p, T) ; \rho = \rho(p, T). \quad (5)$$

With the sudden appearance of damage nature of the flow of air currents in the flow around the external contour of the aircraft may change from laminar to turbulent, especially in the vicinity of the site of injury. For modeling turbulence phenomena there are many mathematical models. Of the large number of turbulence models most widely used turbulence model with two differential equations [9].

In computational hydromechanics (CFD) is widely used k-ε turbulence model, since it has been demonstrated significant advantages over the simpler model in the calculation of a fairly wide class of free and wall turbulent shear flows. In particular, k-ε turbulence model is used in software packages ANSYS FLUENT, Solidworks Flow Simulation, FlowVision et al.

k-ε turbulence model consists of a system of two differential equations: the transport equation of turbulent kinetic energy k, which is a rigorous consequence of the Navier-Stokes equations and the turbulent energy dissipation ε [10, 11]:

$$\frac{\partial}{\partial t}(\rho k) + \frac{\partial}{\partial x_i}(\rho k u_i) = \frac{\partial}{\partial x_i}\left[\left(\mu + \frac{\mu_t}{\sigma_k}\right)\frac{\partial k}{\partial x_i}\right] +$$
$$+ \tau_{ij}^R \frac{\partial u_i}{\partial x_j} - \rho\varepsilon - \mu_t\frac{g_i}{\sigma_B}\frac{1}{\rho}\frac{\partial p}{\partial x_i} \quad (6)$$

$$\frac{\partial}{\partial t}(\rho\varepsilon) + \frac{\partial}{\partial x_i}(\rho\varepsilon u_i) = \frac{\partial}{\partial x_i}\left[\left(\mu + \frac{\mu_t}{\sigma_k}\right)\frac{\partial \varepsilon}{\partial x_i}\right] +$$
$$+ C_1\frac{\varepsilon}{k}\left(f_1\tau_{ij}^R\frac{\partial u_i}{\partial x_j} - C_B\mu_t\frac{g_i}{\sigma_B}\frac{1}{\rho}\frac{\partial p}{\partial x_i}\right) - f_2 C_2\frac{\rho\varepsilon^2}{k} \quad (7)$$

where $f_1, f_2, f_\mu$ – so-called damping functions that for the standard k-ε model are $f_1 = f_2 = f_\mu = 1$; $\tau_{ij}$ – $ij$ – Laminar component of the stress tensor; $\tau_{ij}^R$ – $ij$ Reynolds stress tensor components; $\delta_{ij}$ – Kronecker delta function; $g_i$ – $i$ gravitational component of the projection on the $i$-th axis of gravity; $x_i$ – $i$-th tensor components in the Cartesian coordinate system; $\mu_t$ – turbulent viscosity.

Standard constants k-ε turbulence model: $C_\mu$=0,09; $C_1$=1,44; $C_2$=1,92; $\sigma_k$=1; $\sigma_\varepsilon$=1,3; $\sigma_B$=0,9; $C_B$=1 where $P_B$>0 и $C_B$=0 where $P_B$<0;

Analysis showed that the k-ε model turbulence exists a large number of modifications. In particular, in [12] is proposed to supplement the standard k-ε model damping functions f1, f2, fμ, obtained by semi-empirical. Damping functions f1 and f2 are defined by the following formulas:

$$f_1 = 1 + \left(\frac{0,05}{f_\mu}\right)^3 , \quad f_2 = 1 - e^{R_t^2} \quad (8)$$

Damping function of eddy viscosity is determined by the dependence of fμ:

$$f_\mu = \left(1 - e^{-0,025R_y}\right)^2 \cdot \left(1 + \frac{20,5}{R_t}\right), \quad (9)$$

where in Ry – Reynolds number near the wall, Rt - turbulent Reynolds number of experiment.

### 5. The research results

For the computer simulation program complex SolidWorks Flow Simulation is selected in the following profiles:

– airfoil An-148 at the root of the wing;
– airfoil P-III (15.5 %) (Fig. 2).

Fig. 2. The airfoil TsAGI P-III (15.5 %)

An-148 aircraft wing profile is supercritical (supercritical), with a sharp nose. For this wing flattened profile characterized by the use of properly folded back part, which gives a more even distribution of pressure along the chord profile and thus leads to a shift of the center of pressure back, and increases the critical Mach number by 10–15 %.

Rectangular wing model with the following characteristics:

– the size of the model: 300mm × 300mm.

– extension: 1.

– material - D16T (2024-T3), inside - solid billet.

– parameters of a single injury: an elongated square with a side length of 50 mm, forming a hole in the front edge of the fragment profile perpendicular to the chord.

Turbulence options:

– turbulence intensity of 1 %.

– the turbulent length $4,64 \times 10^{-4}$ m.

For modeling parameters used International standard atmosphere for different heights according to GOST 4401-81.

In the simulation takes into account the following recommendations Support SolidWorks, are based knowledge engineering analysis SolidWorks Simulation Knowledge Base.

The impact velocity of the oncoming flow on the temperature gradient that occurs when damage rectangular shape.

Research of the oncoming flow velocity on temperature gradient was carried out under the following parameter values:

– speed: 40 m / s and 80 m / s, 120 m / s, 160 m / s, 200 m / s, 240 m / s;

– international standard atmosphere (ISA): ambient temperature: 288.2 K (15° C), atmospheric pressure 101 325 Pa (760 mm Hg. Art.) At an altitude of 0 meters above sea level;

– angle of attack α=0 °.

The flow around a rectangular wing profile model AN-148 and temperature distribution under these conditions are shown in Fig. 3-6.

As can be seen from the analysis of Fig. 3, the flow around the damaged part of the local temperature profile in the boundary layer directly damage increases, ie, there is a temperature gradient, which tends to spreading closer to the trailing edge of the model.

Let us analyze the temperature distribution along the upper and lower wing surfaces to distant 1/3 and 2/3 of the front edge of the model (Fig. 4).

Data analysis graphs, shown in Fig. 4, leads to the conclusion that the maximum temperature difference observed in the distance from the leading edge to 1/3 chord and reaches 0.65 K on the upper surface of the model and 0.82 K on the lower plane. The local temperature difference approaches the damage will

increase. At the distance from the leading edge 2/3 chord is also observed fever, but it is uneven distribution, especially on the lower plane of the model, and their difference is less than 0.5 K.

By increasing the speed of the oncoming flow, an increase in not only the local temperature difference between damaged and undamaged areas of the model, but also the area of the spreading of the temperature gradient (Fig. 5, 6). Thus, at a speed of 240 m / s maximum temperature difference on the distance from the leading edge to 1/3 chord is 35 K.
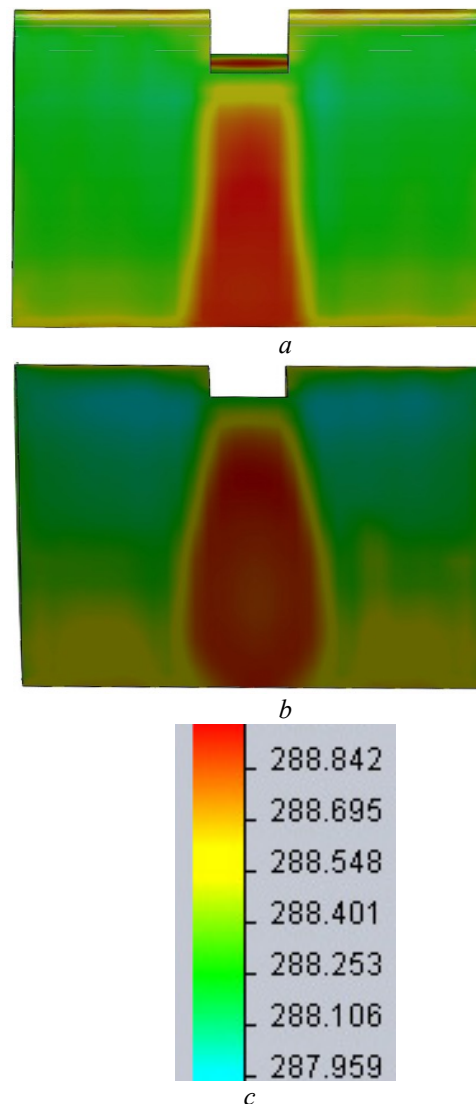


a



b



c

Fig. 3. The temperature gradient that occurs in the boundary layer for damage at the oncoming flow velocity of 40 m / s: a – the upper surface of the rectangular model wing profile-148; b – the lower plane of the rectangular model wing profile-148; c – temperature scale in Kelvin

Analyzing the character shown in Fig. 7 graphs, it is concluded that with increasing speed the local temperature difference between damaged and undamaged areas of the model profile is growing, and its growth is not linear. The growth temperature difference occurs faster on distance from the leading edge to 1/3 chord than the distance from the leading edge 2/3 chord.
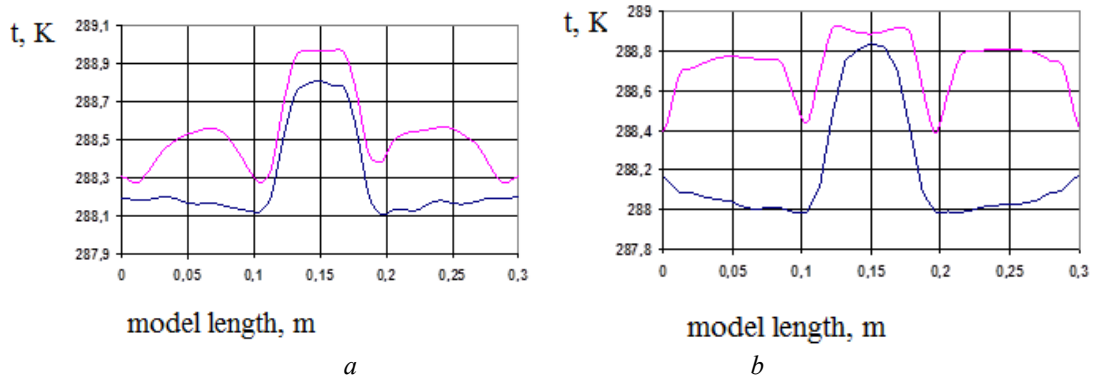
Fig. 4. The temperature distribution along: *a* – the upper boundary layer and *b* – lower surfaces external contour model for oncoming flow velocity of 40 m / s at a distance from the front edge of the 1/3 chord (blue line) and the 2/3 chord (red line)
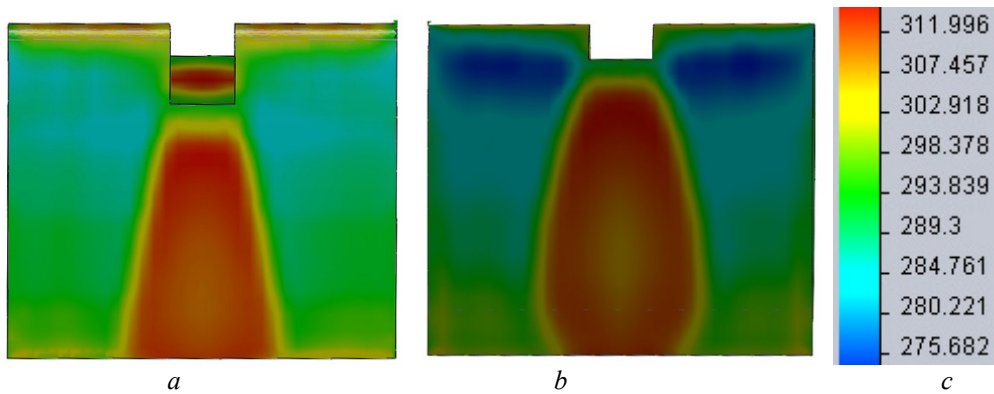


Fig. 5. The temperature gradient that occurs in the boundary layer for damage to the oncoming flow velocity at 240 m / s: *a* – the upper surface of the rectangular model wing profile-148; *b* – the lower plane of the rectangular model wing profile-148; *c* – temperature scale in Kelvin
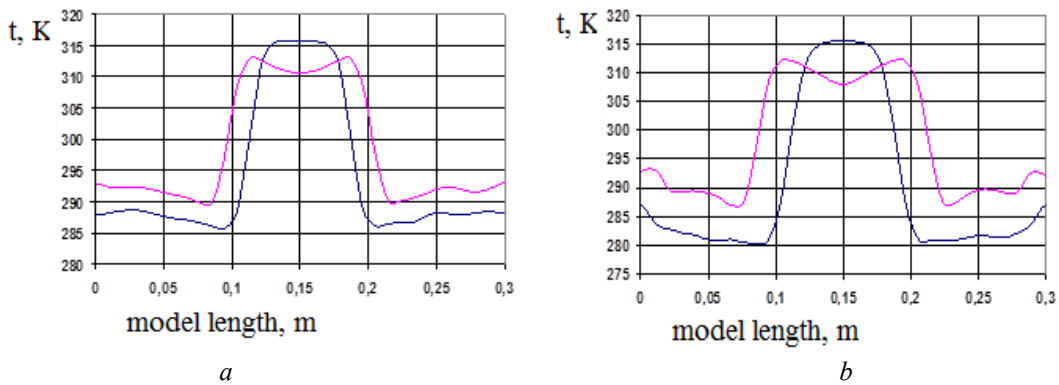


Fig. 6. The temperature distribution along the *a*- upper boundary layer and *b* -lower surfaces external contour model for oncoming flow velocity of 240 m / s at a distance from the front edge of the 1/3 chord (blue line) and the 2/3 chord (red line)
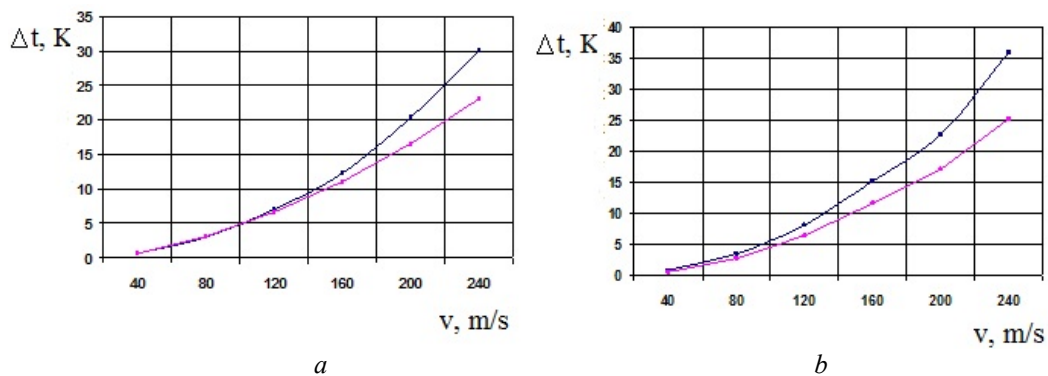


Fig. 7. Dependence of the local temperature difference between damaged and undamaged areas of the model profile of oncoming flow velocity on the *a* – upper surface profile  and *b* – the lower plane of the profile the distance from the leading edge to 1/3 chord (blue line) and 2 / 3 chords (red line)

Hence, at a speed of 40 m/s local temperature difference on the distance from the front edge of the 1/3 chord higher than the distance from the leading edge 2/3 chord at 0.3 K along the upper surface and at 0.4 K along the bottom plane model. And at a speed of 240 m/s, these figures are 6.5 K and 10 K, respectively.

So, if you have the means to measure the temperature can detect temperature differences of damaged and undamaged areas of the outer contour, placing meters far from the leading edge of the lower 1/3 of the chord plane model or close to the site of injury at a speed of 40 m/s.

Impact damage location on the temperature gradient, arising from damage.

Study of fault location on the temperature gradient was carried out under the following parameter values:
– oncoming flow velocity: 100 m / s.

– international standard atmosphere (ISA): ambient temperature: 288.2 K (15 ° C), atmospheric pressure 101 325 Pa (760 mm Hg. Art.) At an altitude of 0 meters above sea level.
– angle of attack.
– the distance from the leading edge to the front edge damage: 25 mm, 125 mm and 225 mm.

The results of studies of the impact location of the damage to the temperature gradient at a distance from leading edge prior to the damage of 25 mm are shown in Fig. 8, 9.

As follows from the analysis of the simulation results (Fig. 8, 9), the distance from the leading edge to the beginning of the damage to 25 mm, the local temperature difference is smaller than the leading edge damage at the same amounts of damage. In addition, a decrease of about 1 K in all cases.
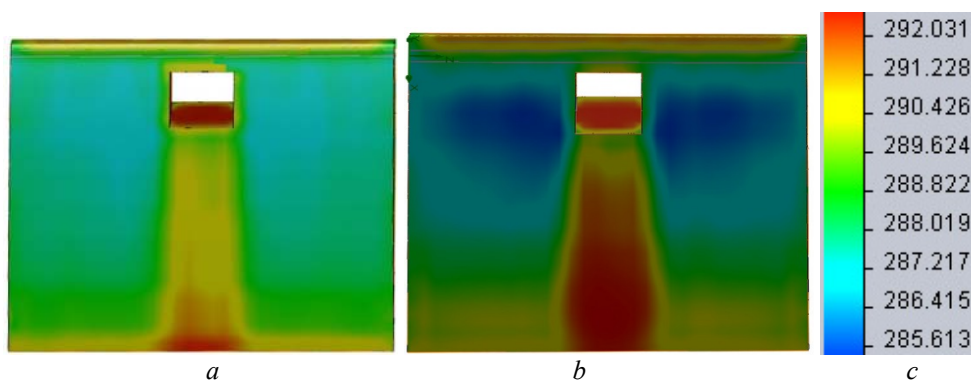


Fig. 8. The temperature gradient that occurs in the boundary layer for damage at a distance from the leading edge to the top damage 25 mm: *a* – the upper surface of the rectangular model wing profile-148; *b* – the lower plane of the rectangular model wing profile-148; *c* – temperature scale in Kelvin
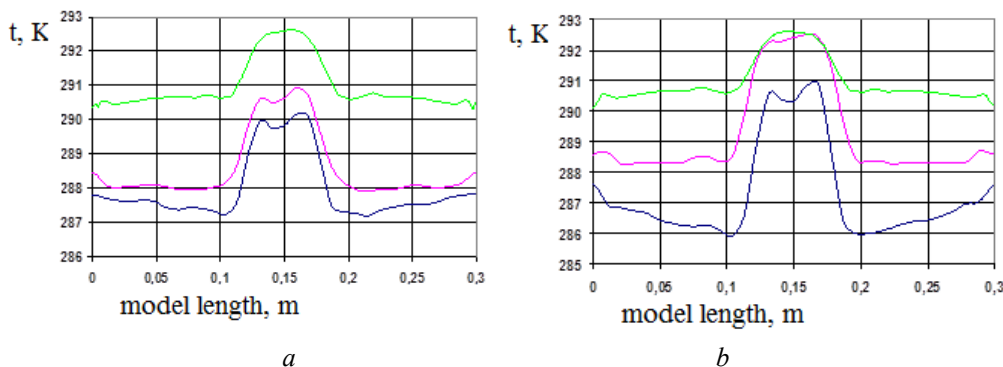


Fig. 9. Distribution of the temperature boundary layer along the *a*- top and *b*- lower surfaces external contour model at a distance from the leading edge to the top damage 25 mm distance from the leading edge to 1/3 chord (blue line), 2/3 chord (red line) and the trailing edge of the profile (green line)

Thus we can conclude that the maximum temperature difference is: along the upper surface of the outer contour far from the leading edge to 1/3 chord – 3.4 K, 2/3 chord – 3 K; along the lower plane of the outer contour far from the leading edge to 1/3 chord – 5 K 2/3 chord – 4 K.

Found that the distance from the leading edge to the beginning of the damage of 125 mm (Fig. 10, 11) the maximum local temperature difference again shows a tendency to decrease, to 2.5 K at a distance from the front edge of the 2/3 chord along the upper surface of the outer contour and 3 K along the lower plane.

In addition, the local temperature difference in the vicinity of the trailing edge of the profile remains almost unchanged and is - on top of – 1.5 K, on the bottom – 1 K. spreading temperature gradients are observed along the upper surface of the rectangular model wing profile and has a slight spreading along the bottom plane.

In the event of damage to the distance from the leading edge to top border damage 225 mm (Fig. 12, 13), it is clear that the local temperature difference in the vicinity of the trailing edge of the profile and is slightly increased – along the upper surface of - 2.5 K along the lower plane – 1.5 K.
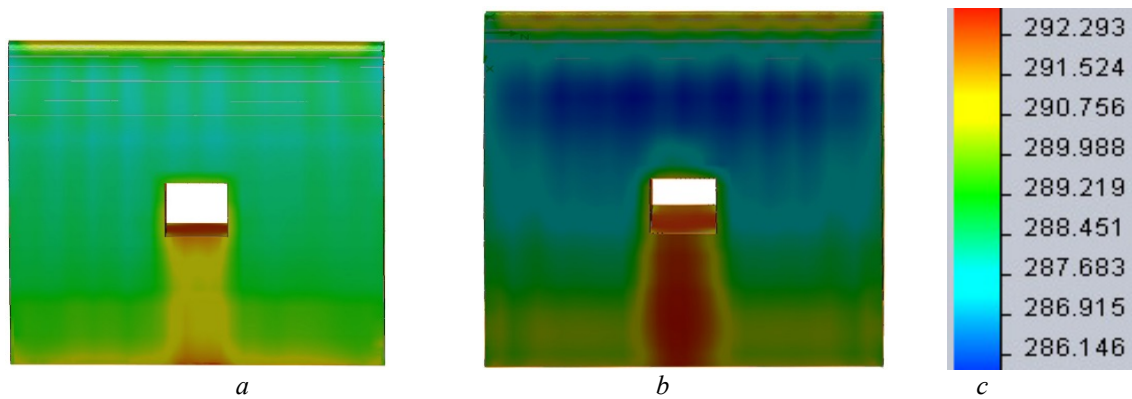
Fig. 10. Temperature gradient that occurs in the boundary layer for damage at a distance from the leading edge to the top 125 mm of damage: *a* – the upper surface of the rectangular model wing profile-148; *b* – the lower plane rectangular wing profile model AN-148; *c* – temperature scale in Kelvin
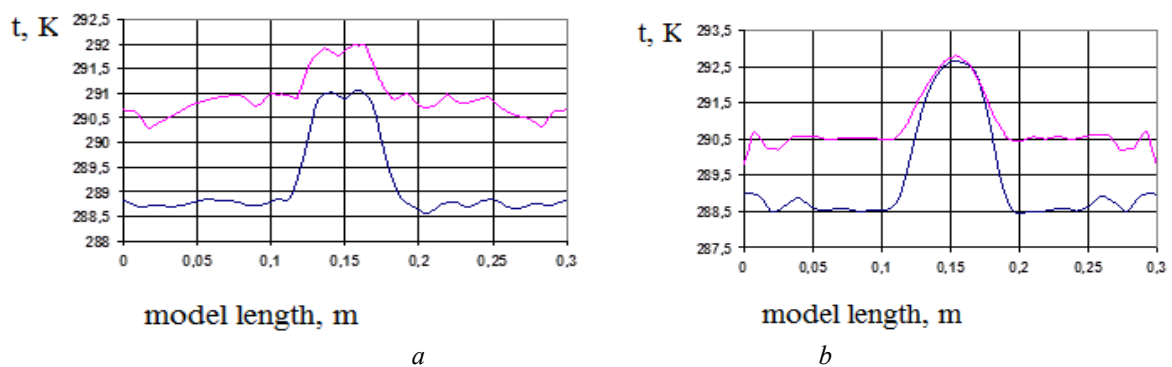


Fig. 11. Distribution of the temperature boundary layer along the *a*- top and *b*- lower surfaces external contour model at a distance from the leading edge to the beginning of damage 125 mm far from the leading edge 2/3 chord (blue line) and the trailing edge of the profile (red line)
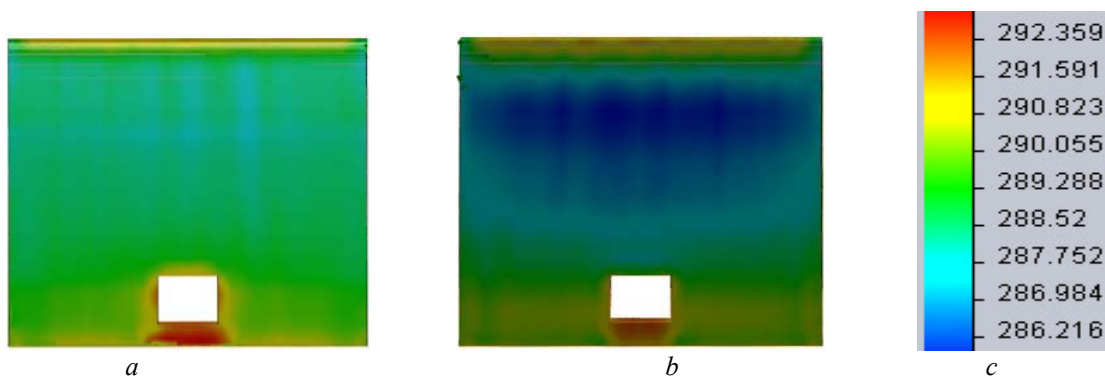


Fig. 12. The temperature gradient that occurs in the boundary layer for damage at a distance from the leading edge to the top 225 mm of damage: *a* – the upper surface of the rectangular model wing profile-148; *b* – the lower plane of the rectangular model wing profile-148; *c* – temperature scale in Kelvin
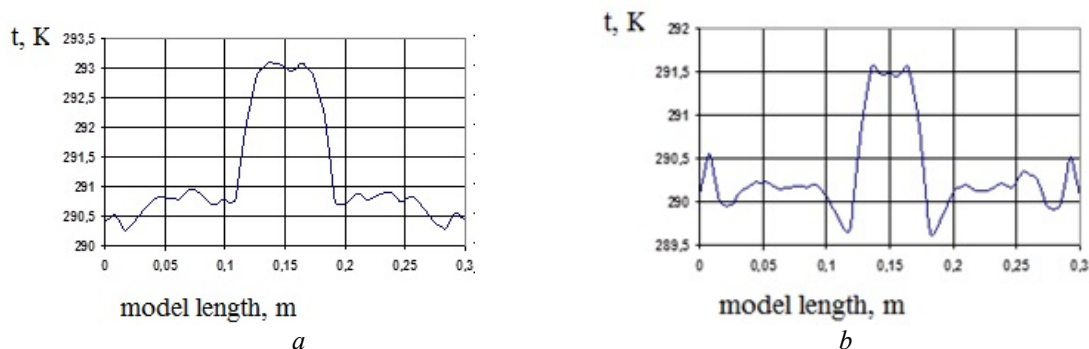


Fig. 13. Average temperature boundary layer along the *a*- top and *b*- lower surfaces external contour model with distance from the leading edge to the beginning of damage 225 mm at the rear edge profile

## 6. Conclusions

In the paper the influence of the speed and angle of attack of the aircraft on the temperature gradient that occurs due to damage of rectangular shape the external contour of the wing aircraft An-148. From the analysis of the results shows that the difference in temperature between the damaged and undamaged portions of the external contour is influenced by the speed and angle of attack. With increasing speed of 40 m/s to 240 m/s the temperature difference increases, along the line remote from the leading edge chord 1/3 and 2/3 of the chord on the upper plane of the external contour from 30 K and 0,7 K to 0 , 7 K to 23 K, respectively. At the bottom of the external contours of the difference in temperature also tends to increase along the line remote from the leading edge chord 1/3 and 2/3 of the chord from 0,85 K to 36 K and from 0,53 K to 25,2 K respectively.

When approaching the critical angle of attack to the observed phenomenon is spreading plume temperature, ie, schedules become flatter. Due to the increase in the area of spreading thermal plume is extremely difficult to determine the date, place and degree, at angles of attack less than -15° – along the upper surface of the external contour, at angles of attack greater than 15° – along the bottom plane of the external contour. In this case for all the other angles of attack for a speed of 100 m/s temperature difference along the lines of 1/3 and 2/3 chord chord varies from 1.5 K to 6 K, which together with the nature of the spreading plume temperature makes it possible to determine the time, place and degree of damages on the basis of thermal fields contours.

It should be noted that as a result of airflow external contour aircraft in flight distribution of temperature along the external contour has a heterogeneous nature. Most of the heated portion of the intact wing is the leading edge of the wing through the critical point of flow separation. With increasing speed increases convective heat flux along the upper and lower planes of the external contour that is caused by the phenomenon of aerodynamic heating. With the change of position of the critical point, the consequences of the change in the angle of attack, the distribution of temperature fields along the wing changes, but the absolute value of the difference between the temperature remains constant.

Changing the geometrical shape of the wing at the entry of foreign forces in most cases leads to a violation of the nature of flow, further turbulence and flow separation due to damage. When turbulence flow significantly increases the intensity of heat transfer processes in the boundary layer, as well as the inhibition of the flow at the site of damage, all of which leads to a temperature gradient of the damage. The intensity of the temperature gradient and the temperature difference increases with increasing flying speed, area of spreading gradient remains practically unchanged. When you change the angle of attack changes the position of the critical point, which leads to an increase in the spreading of the temperature gradient, the intensification of heat transfer processes in the boundary layer along one of the planes with simultaneous drop another, ie to a redistribution of temperature fields on the wing.

The choice of transducers for the possibility of diagnosing the external contour of the aircraft in flight. It is shown that the most advisable to use a thermocouple type TMKn accuracy class 1 (±0.5 K), which allow to catch the temperature difference between the damaged and undamaged portions of the external contour at a speed of 40 m/s, the component 0,58 K. Shows the structure of the sensor designed for placement directly on the outer side of the aircraft, which does not disturb the airflow along the wing.

The temperature Reynolds number, which relates the temperature difference between the undisturbed air environment with a temperature difference between the damaged and undamaged portions of the external contour of the aircraft in flight, and flight altitude with the magnitude of damage to the wing chord. For the dependence of the angle of attack, which relates the change in the lift with the change in the area of the wing as a result of damage to the temperature difference and damaged and undamaged portions of the outer contours.

The results obtained can be used when creating a system of diagnosing the state of the external contour of the aircraft in flight based on their thermal fields.

### References

1. Wildlife, E. (2005). Strikes to Civil Aircraft in the United States 1990-2004. Federal Aviation Administration National Strike Database, 11, 77.

2. Allan, J. et. al. (2001). The Costs of Birdstrikes to Commercial Aviation. Bird Strike Committee Proceedings, Bird Strike Committee USA. Canada, Third Joint Annual Meeting. Calgary, AB, 10.

3. Blair, A. et. al. (2008). Blair Aeroengine Fan Blade Design Accounting for Bird Strike. A thesis submitted in partial fulfillment of the requirements for the degree of Bachellor of Applied Science. Department of Mechanical and Industrial Engineering. The University of Toronto, 84.

4. Accident and Serious Incident Reports: Bird Strike. Available at: http://www.skybrary.aero/index.php/ Accident_and_Serious_Incident _Reports: _BS

5. Shevchuk, D. O. (2013). Automated identification system baseds on the changing of the temperature field of aircraft elements. Electronics and control systems, 4 (38), 114–118. [in Ukraine]

6. Schlichting, H. (1974). Boundary layer theory. Moscow: Nauka, 713. [in Russian]

7. Avduevskii, V. et. al. (1992). Fundamentals of heat transfer in the aviation and space technology. Moscow: Mechanical Engineering, 528. [in Russian]

8. Weigand, B. (2004). Analytical Methods for Heat Transfer and Fluid Flow Problems. Springer, 263.

9. Wilcox, D. (1994). Turbulence modeling for CFD, DCW Industries. Inc., 477.

10. Wilcox, D. (1988). Multiscale Model for Turbulent Flows. AIAA Journal, 26 (11), 1311–1320. doi: 10.2514/3.10042

11. Enhanced turbulence modeling in Solidworks Flow Simulation (2013). Dassault Systemes, 21.

12. Lam, C. (1981). Modified Form of the k-ε Model for Predicting Wall Turbulence. Journal of Fluids Engineering, 103 (3), 456–460. doi: 10.1115/1.3240815

**Vasyl Kazak,** doctor of Technical Sciences, professor, Automation and Energy Management Department, National Aviation University, Komarova Ave, 1, Kiev, Ukraine, 03058
E-mail: profkazak@ukr.net
**Dmitro Shevchuk**, PhD, associate Professor, Automation and Energy Management Department, National Aviation University. Komarova Ave, 1, Kiev, Ukraine, 03058
E-mail: dmitroshevchuk@gmail.com
**Andrii Babenko**, PhD, assistant professor, Air Transportation Management Department
National Aviation University, Komarova Ave, 1, Kiev, Ukraine, 03058,
E-mail: andrii.babenko@gmail.com
**Mykhailo Levchenko**, student, Department of Automation and Energy Management, National Aviation University, pr., Komarova 1, Kyiv, Ukraine, 03058,
E-mail: mhlevchenko@gmail.com

# ПРИМЕНЕНИЕ ИНФОРМАЦИОННЫХ ТЕХНОЛОГИЙ ПРИ СИНТЕЗЕ МЕТОДОВ ОЧИСТКИ ДАННЫХ

## © В. А. Доровской, С. Г. Черный, И. А. Доровская, Н. П. Сметюх

*Осуществлен анализ методов очистки данных мониторинга условий труда; изложены общие принципы и алгоритмы методов очистки данных. Для технологии по очистке данных использование пакетов MICROSOFT SQL SERVER и MATLAB дает положительные результаты, но имеет определенные преграды. В связи с этим возникает необходимость разработки компьютерных промышленных открытых пакетов по методам очистки данных.*
*Ключевые слова: очистка данных, идентификация, кластеризация, data mining, консолидация, SQL, горно-металлургический, эксперт.*

*The analysis of methods for monitoring data cleansing of working conditions is proved; the general principles and methods of data cleaning algorithms are given. Usage of MICROSOFT SQL SERVER and MATLAB gives positive results for data cleansing technology, but it has some obstacles. In this regard, there is a need to develop the industrial computer open packages of data cleansing methods.*
*Keywords: data cleansing, identification, clustering, data mining, consolidation, SQL, ore mining and smelting, expert.*

### 1. Введение

Горно-металлургические предприятия гиганты (горно-обогатительные комбинаты, металлургический комбинат, подземный горнодобывающий комбинат) (ГМП)), которые характеризуются большими объемами производства с использованием значительных человеческих ресурсов, требуют новых ИТ-технологий управления методами очистки данных мониторинга условий труда горно-металлургических рабочих (ГМР) [1, 2]. Мониторинг условий труда ГМР позволяет осуществлять накопление данных оценки УТ с целью дальнейшего использования этих данных при формировании состава пенсионного списка ГМР.

В работе исследуется проблема ИТ-технологий управления методами очистки данных мониторинга УТ ГМР. Актуальность этой проблема очевидна потому что, количество ГМР работающих в очень тяжелых УТ ежегодно увеличивается (табл. 1), что приводит к истощению человеческих ресурсов региона.

### 2. Анализ литературных источников по очистке данных

Горно-металлургические предприятия относят-ся

к сложным динамическим системам [1] и имеют следующие отличительные особенности данных УТ РМ:

– непостоянство РМ;

– необходимость строгого соблюдения планов по выполняемым в определенное время объемам;

– большая зависимость результатов функционирования от природных условий (геологических и климатических);

– трудности в организации функционирования системы постоянно перемещающихся РМ.

С позиции системных компонентов можно выделить: наличие большого количества случайных факторов УТ РМ и трудности прогнозирования протекания технологических процессов, и функционирования всей системы на длительный промежуток времени. С точки зрения аналитического составляющего, заметим, что возникает существенная проблематика в осуществлении автоматизированного управления производственными процессами по причинам непостоянства РМ и отсутствие, необходимых для контроля датчиков, средств передачи информации на управляющий центр, а так же неравномерный режим работы оборудования на протяжении смены и количество данных (табл. 1).